COMMUNICATION

2,4,6-Trinitrotoluene (TNT) Chemical Sensing Based on Aligned Single-Walled Carbon Nanotubes and ZnO Nanowires

By *Po-Chiang Chen, Saowalak Sukcharoenchoke, Koungmin Ryu, Lewis Gomez de Arco, Alexander Badmaev, Chuan Wang,* and *Chongwu Zhou**

Chemical sensors based on one-dimensional (1D) nanostructures have attracted a great deal of attention because of their exquisite sensitivity and fast response to the surrounding environment.[1–5] In addition, both carbon nanotubes and metal oxide nanowires are promising candidates for building an electronic nose (e-nose) system.[6,7] Among these materials, semiconductor single-walled carbon nanotubes (SWNTs) are molecular-scale wires composed entirely of surface atoms, which should be ideal for the direct electrical detection and are expected to exhibit excellent sensitivity to surrounding chemical and biological species.[8–10] Kong et al. initially utilized SWNT field-effect transistors (FETs) to detect nitrogen dioxide (NO_2) and ammonia (NH_3), and demonstrated a detection limit of 2 ppm for NO_2 and 0.1% for NH_3.[11] Subsequently, such SWNT-based chemical sensors have been applied to detect a wide variety of chemicals and the detection limits have been significantly improved. Qi et al. fabricated large arrays of functionalized SWNT sensors, and the detection limit of NO_2 was lowered to 100 ppt.[12] In addition, metal oxide nanowires have been widely studied and demonstrated with great potential for chemical sensing applications.[13–16]

Recently, due to the threat of terrorism and the need for homeland security, significant progress has been achieved in the detection of both explosives and nerve agents, such as 2,4,6-trinitrotoluene (TNT), 2,4-dinitrotoluene (DNT), hexogen (DRX), and dimethyl methylphosphonate (DMMP).[17–20] One of the leading candidates is 1D nanostructure-based chemoresistors or FETs. Snow et al.[21] and Wang et al.[22] have reported the detection of DMMP at ppb level by using SWNT and SnO_2 nanowire-based chemical sensors, respectively. However, to our knowledge, there were only a few reports on the use of 1D nanostructure-based chemoresistors and FETs for detecting explosives, and the detection mechanism is still unclear.[23,24]

In addition, electronic devices fabricated on mechanically flexible substrates have recently attracted enormous attention, due to the proliferation of handheld applications in portable electronics, aerospace science, and civil engineering. Currently, conventional microfabrication techniques or printing methods can be applied to SWNTs on plastic substrates to form devices, allowing inexpensive mass-production and conformable electronics.[25–27]

In this paper, we report the transfer of aligned semiconductor SWNTs onto cloth fabric and successful fabrication of flexible SWNT chemical sensors, which have great potential for wearable electronics. These SWNT chemical sensors exhibited good sensitivity of trace chemical vapors, including 8 ppb TNT and 40 ppb NO_2, at room temperature. Besides, to realize the concept of an electronic nose (e-nose) system for explosives, we also fabricated ZnO nanowire-based chemical sensors, which showed a detection limit of 60 ppb for TNT molecules at room temperature. To our knowledge, this is the first TNT sensor built on the basis of metal oxide nanowires. In addition, the detection limit of our chemical sensors is close to the limit of 1.5 ppb TNT set by the U.S. Occupational Safety and Health Administration. The flexible TNT sensors can find immediate applications in systems that demand mechanical flexibility, light weight, and high sensitivity.

The fabrication of flexible SWNT chemical sensors started with the synthesis of SWNTs on quartz substrates using a chemical vapor deposition (CVD) method, which have been reported by us and other groups.[28–30] After growth, we adapted a facile method[31] to transfer the aligned nanotubes from the original substrate to fabric. In brief, a 100-nm-thick gold film was first deposited on the original substrate with aligned SWNTs, followed by applying a thermal tape to peel off the gold film and nanotubes from the growth substrate. The gold film with SWNTs on the thermal tape were pressed against a piece of textile fabric, which was pre-coated with polyethylene at elevated temperature and then transferred from thermal tape onto textile fabric, which had a 50-nm Ti layer as back-gate electrode and 2-μm-thick SU-8 as gate dielectric layer. The thermal tape was released, and KI/I_2 gold etchant was then applied to remove gold films. Finally, Ti (0.5 nm) and Pd (40 nm) were deposited on the transferred SWNTs as source/drain electrodes. A schematic diagram of a flexible SWNT chemical sensor is shown in Figure 1a.

Figure 1b shows an optical photograph of flexible aligned SWNT FETs on a textile fabric. It can be clearly seen from the SEM image (right) that the nanotubes bridge the two electrodes. Figure 1c displays the current–gate-voltage (I–V_g) characteristics of a typical flexible transistor on fabric before and after electrical breakdown. The device showed significant improvement for the

[*] Prof. C. Zhou, P.-C. Chen, S. Sukcharoenchoke, K. Ryu, L. Gomez de Arco, A. Badmaev, C. Wang
Ming Hsieh Department of Electrical Engineering
University Southern California
Los Angeles, CA 90089 (USA)
E-mail: chongwuz@usc.edu

DOI: 10.1002/adma.200904005

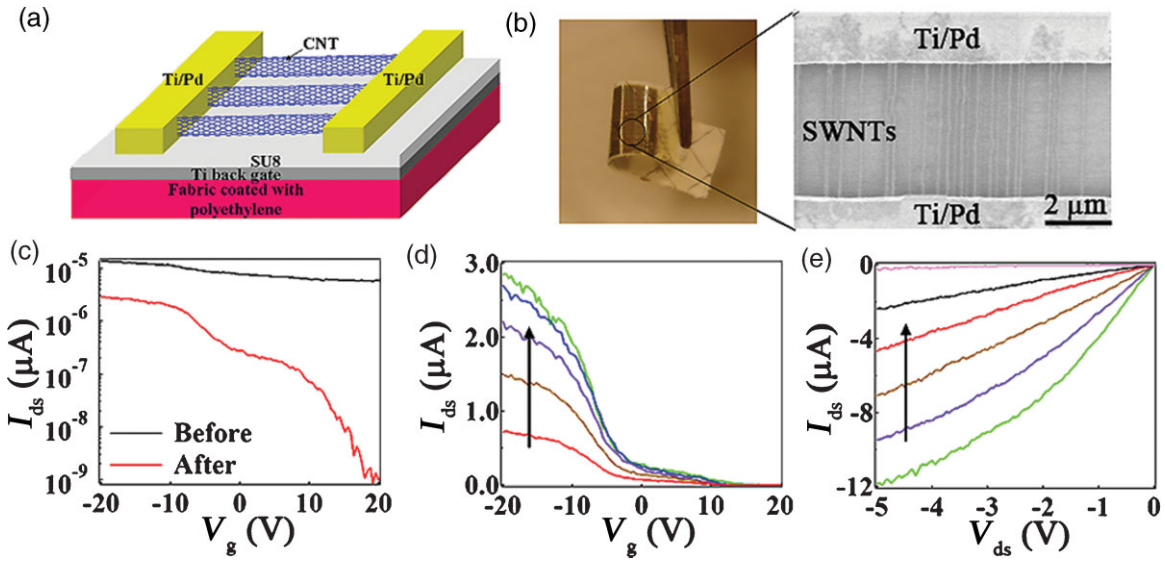

Figure 1. Wearable transistors based on aligned nanotubes transferred to fabric. a) Schematic diagram showing a transistor structure that uses polyethylene-coated fabric as the substrate, 50-nm Ti film for the back-gate electrode, 2-μm SU-8 as the dielectric layer, and the transferred aligned nanotube array as the active channel. b) The optical microscopy image showing an array of such transistors built on a flexible fabric. c) I–V_g curves of a transistor ($L = 4$ μm, $W = 10$ μm, $D = \sim 2$ tubes/μm) before and after electrical breakdown. d) I–V_g curves at different V_{ds} for the device in (c). V_{ds} is varied from −0.2 to −1 V in steps of −200 mV. (e) I–V_{ds} curves at different V_g for the same device in (c). The curves correspond to V_g ranging from +10 to −20 V in step of −5 V.

on/off ratio from 2.3 to 3×10^3, accompanied by a decrease of the on-state current due to metallic carbon nanotube removal. After electrical breakdown, further I–V_g and current vs. drain-source-voltage (I–V_{ds}) measurements were also carried out. Figure 1d shows the current magnitude ($|I|$) as a function of the gate voltage (V_g) at different V_{ds} from −0.2 to −1 V with a step of −200 mV, showing a pronounced p-type semiconductor behavior. We extracted the subthreshold swing of this device to be 2 V/decade and the on/off ratio as high as 10^5. In addition, Figure 1e shows a set of I–V_{ds} curves at different gate voltages. The highest current obtained at $V_g = -20$ V and $V_{ds} = -5$ is 11.8 μA, and the device also showed moderate current saturation behavior. Our results are comparable with early reported work on both rigid and flexible substrates.[31,32]

The chemical sensing experiments were performed using a home-made chemical sensing setup described in our previous work.[33–38] Briefly, the as-prepared flexible SWNT sensors were mounted on a chip carrier inside a sealed chamber with an electrical feedthrough and gas inlet/outlet. The TNT vapor was generated from TNT powder (99.0%, Chem Service) with/without heating, and air was used as carrier gas in the experiments. The details for the estimated TNT concentrations can be found in the Supporting Information. In order to simulate the practical environment, some parts of the gas line were exposed to indoor light. Figure 2a displays the I–V curves (at $V_g = 0$ V) obtained under different TNT concentrations of 0.15, 0.4, and 0.6, and 5 ppm NO_2 as a comparison. These curves are found to be rather linear and indicate the Ohmic contact nature for the sensing devices in diluted TNT and NO_2 environment. With the increasing TNT concentration, the device conductance was monotonically suppressed from 3 μS (in air) to 2 μS (in 0.6 ppm TNT). On the other hand, the device conductance was increased to 4.2 μS while the device was exposed to 5 ppm NO_2. The NO_2, known as a strong electron-withdrawing compound, is expected to increase the hole concentration in p-type nanotubes, thus leading to the observed higher conductance. Besides, a sensing experiment of six sensing cycles with six different NO_2 concentrations ranging from 40 ppb to 5 ppm has been carried out and can be found in the Supporting Information. Figure 2b plots the change in SWNT conductance normalized by the initial conductance at gate bias $V_g = 0$ V for TNT sensing. Eight cycles have been successively recorded, corresponding to eight different TNT concentrations ranging from 8 ppb to 1.1 ppm, respectively. The relative sensor response (RS) in conductance is defined as

$$RS = \frac{\Delta G}{G_0} = \frac{G - G_0}{G_0} \quad (1)$$

where G_0 and G denote the nanotube conductance before and after the exposure, respectively.

Each cycle of sensing was started by desorbing the attached molecules with ultraviolet (UV) light ($\lambda \sim 254$ nm) irradiation (at the point A, taking the first cycle as an example), as previously demonstrated.[39] The SWNT conductance kept increasing until the UV light was turned off at point B. The conductance decreased gradually, due to the electron-hole recombination and re-adsorption of oxygen molecules and moisture in the air. After a relatively stabilized state was reached, diluted TNT vapor (TNT in air, 8 ppb) was introduced to the airflow at point C. The lowest detectable TNT concentration was found to be ~8 ppb in air. With higher concentration TNT used, more pronounced conductance modulation was observed, as shown in Figure 2b. Figure 2c shows a linear dependency between the normalized sensor response and

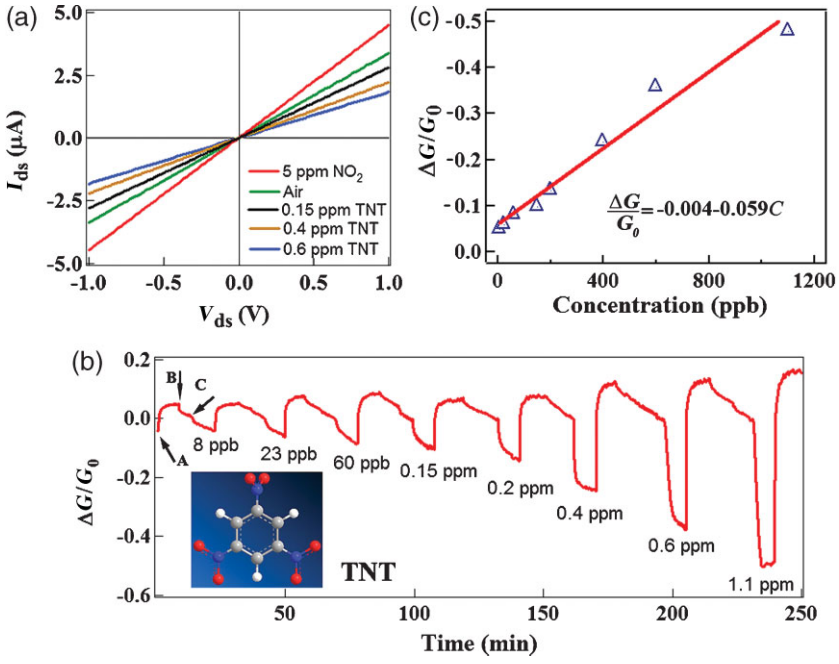

Figure 2. a) *I–V* curves taken in air, 5 ppm NO_2, and three different TNT concentrations. b) Sensing response of a flexible SWNT sensor to TNT. The normalized conductance change ($\Delta G/G_0$) is plotted as a function of time with the sensor exposed to TNT of different concentrations. Recovery was made by UV light (254 nm). The inset shows TNT structure. c) Plot of $\Delta G/G_0$ vs. the TNT concentration.

the TNT concentration, which can be fitted as $\Delta G/G_0 = -0.004–0.059C$. The reduced conductance we observed for the SWNT sensors under TNT exposure is interesting, and will be further discussed below based on the results of positive ion mass spectrometry. We note that reduced conductance was previously reported for DNT sensing using SWNT networks and reduced graphene oxides,[22,40] but no previous report can be found on the effect of TNT exposure on SWNT conductance. In addition, TNT molecules are easy to decompose into small molecular fragments under light illumination or heat treatments, which might influence the sensing behaviors of SWNTs.[40] As a result, our wearable SWNT-based sensing devices showed good sensitivity to TNT at room temperature, and the detection limit is comparable with the conductive polymer TNT sensors.[41]

To further investigate the TNT sensing mechanism, we have also studied the effect of TNT on ZnO nanowire sensors, which would be essential components to be combined with carbon nanotube sensors for electronic nose systems.[6] Figure 3a shows a schematic diagram of a ZnO nanowire sensor. The synthesis of ZnO nanowire and device fabrication can be found in the Supporting Information. The SEM image (inset of Fig. 3a) reveals the dimension of a single ZnO nanowire sensor with the channel length of 2 μm. The *I–V* curves (at $V_g = 0$ V) obtained under the different TNT concentrations from 60 ppb to 1.36 ppm are shown in Fig. 3b. With increasing TNT concentration, the device conductance was monotonically suppressed from 3 μS (in air) to 0.5 μS (in 1.36 ppm TNT). Figure 3c plots the changes in ZnO nanowire conductance normalized against the initial conductance. Seven cycles have been successively recorded, corresponding to seven different TNT/air concentrations ranging from 60 ppb to 1.36 ppm, respectively. Similar to semiconductor SWNTs, with increasing TNT concentration, more pronounced conductance modulation was observed. The lowest detectable concentration is ~60 ppb for a ZnO nanowire sensor. To our knowledge, this is the lowest detection limit reported so far using metal oxide nanowire based chemical sensors to detect TNT.

Figure 3d plots the derived normalized sensor response as a function of TNT concentrations (*C*). The curve is rather linear at low TNT concentration (<200 ppb), but tends to saturate when the TNT partial pressure went up. This curve can be well

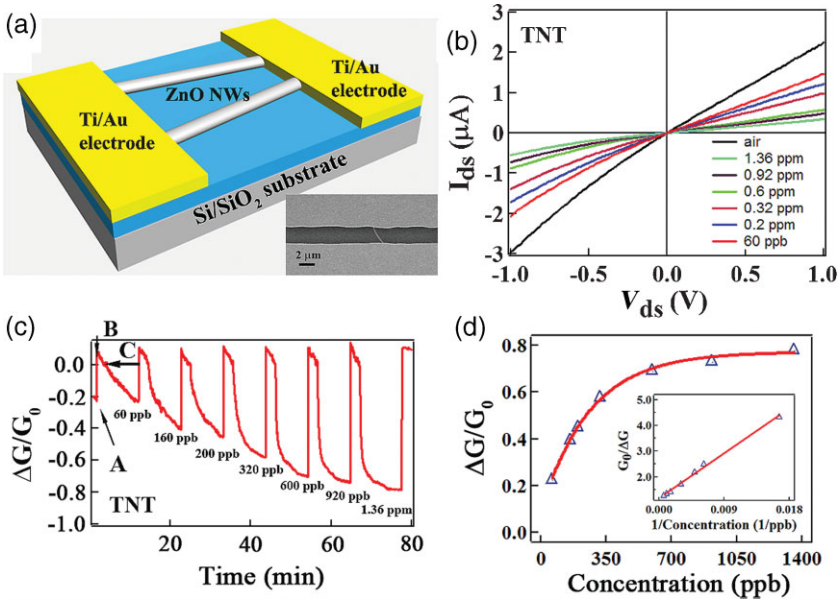

Figure 3. a) Schematic view of a ZnO nanowire transistor structure, with Ti/Au deposited on ZnO nanowires as source and drain electrodes. Inset: SEM image of the as-fabricated ZnO nanowire chemical sensor. The scale bar is 2 μm. b) *I–V* curves taken in air and at different TNT concentrations. c) Sensing response of a ZnO nanowire chemical sensor to TNT. The normalized conductance change ($\Delta G/G_0$) is plotted as a function of time with the sensor being exposed to TNT of different concentrations. d) Normalized conductance change ($\Delta G/G_0$) vs. TNT concentrations (*C*), which was fitted using $S = 1/(A + B/C)$. Inset: *1/S* vs. *1/C* with linear line fit.

fitted with the following equation:

$$\frac{\Delta G}{G_0} = \frac{A}{1+\frac{B}{C}} \quad (2)$$

with $A = 0.086$ and $B = 16.74$, which has also been further confirmed by the linear fitting of RS^{-1} and C^{-1} shown in the inset of Figure 3d. The results can be understood as the surface coverage of adsorbed molecules follows Langmuir isotherm.[33] At lower concentrations, the chemical sensor exhibited a linear dependence between the normalized sensor response and the TNT concentration. At higher concentrations, the surface coverage tends to saturate and hence leads to the saturation response observed in Figure 3d. In comparisons of ZnO nanowire based TNT sensors, SWNT based sensors did not exhibit a saturation response at the higher TNT concentrations (shown in Fig. 2c). We tentatively attributed this difference to the varied SWNT and nanowire density in our sensing devices. For SWNT chemical sensors, the transferred carbon nanotube density was about 4 tubes/μm in average (channel width is 50 μm), which provided a lot of reaction sites for TNT molecules and resulted in the unsaturated behavior at high TNT concentrations. On the other hand, the ZnO nanowire chemical sensors, with nanowire density less than 1 wire/μm, provided less reaction sites for TNT molecules than SWNT chemical sensors and could saturate easily at high TNT concentrations.

Since the TNT molecule decomposition process is complex, more detailed experiments are required to understand the surface adsorption behavior of TNT and its decomposition products. For this purpose, a positive ion mass spectrometer (Omnistar, GSD 310O, Pfeiffer) with an ion beam intensity of 70 eV was connected to the sensing chamber. A standard mass spectrum of air at 25 °C is shown in Figure 4a. We can see a typical electron ionization (EI) mass spectrum of air with a base peak at m/z 40 due to the presence of argon ions (Ar^+). Major ions in the mass spectrum of air are at m/z 28 (N_2), m/z 32 (O_2), m/z 34 (hydroxyl group), and m/z 44 (CO_2). The peaks located between m/z 14 and m/z 22 can be attributed to the second ionization energy of N_2, O_2, hydroxyl group, and CO_2 in air. These characteristic air peaks can be used as a reference for the identification of TNT molecules. Figure 4b shows the mass spectrum of 23 ppb TNT in air. As one can observe in the inset of Figure 4b, in comparison to the mass spectrum of air, there are two additional peaks in the spectrum, including NO molecules (m/z at 30) and NO_2 molecules (m/z at 46). NO molecule is a well-known electron donor to SWNTs, and is a signature decomposition product of TNT molecules because of the photolysis occurring under the experimental conditions.[42,43] The NO_2 molecule is known as an electron-withdrawing group. However, the ratio between NO and NO_2 is estimated to be 20, which is consistent with previous publications that report that NO is the most abundant product from TNT decomposition. Our results suggest that the reduction in nanotube conductance is induced by the abundance of NO relative to NO_2 in the decomposition products of TNT. In addition to NO and NO_2, there are other decomposition products in the sensing chamber that might influence the electron or hole concentrations in sensing materials, such as nitrobenzene, RDX, nitromethane, and DNT,[40,44] which are beyond the detection limit of our mass spectrometer.

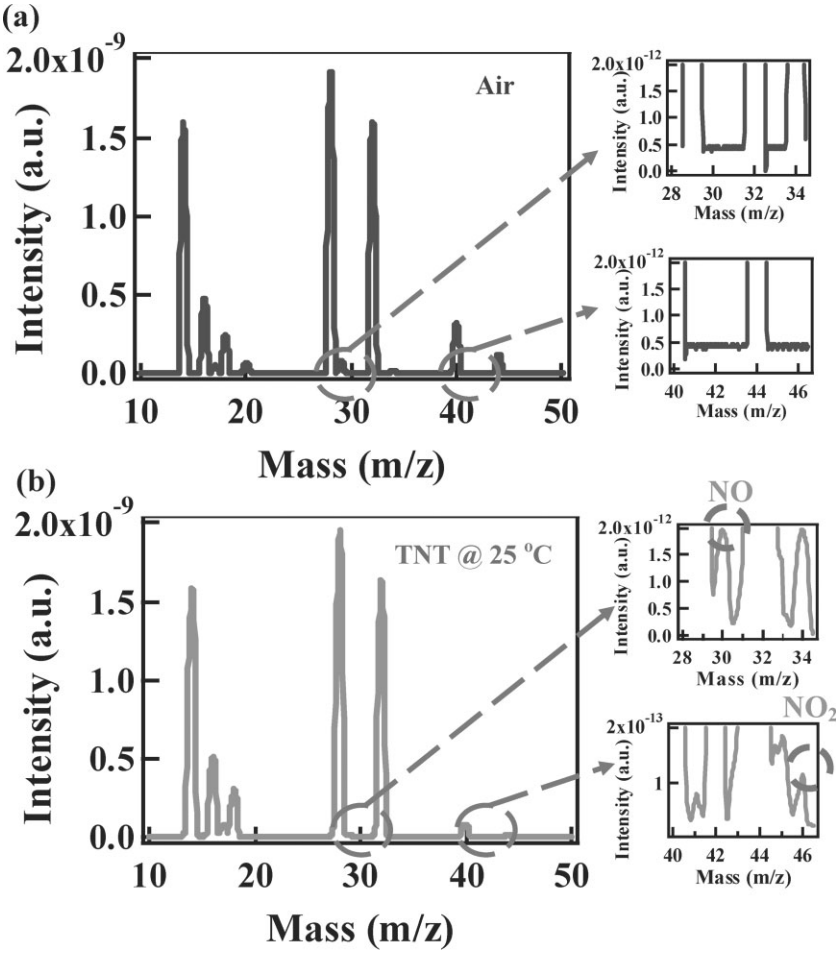

Figure 4. Positive ion mass spectrum of a) air and b) 23 ppb TNT in air, recorded at an electron energy of 70 eV.

On the other hand, for ZnO nanowire sensors, the dominant mechanism[45] is that NO can react with oxygen ions on the metal oxide surface and convert to NO_2 (shown in Equation 3 below).[45] The adsorbed NO_2 molecules are strongly electron-withdrawing, and thus cause a reduced conductance for ZnO nanowire sensing devices, consistent with our observation reported in Figure 3.

$$NO + O^-_{2\,\text{surface}} + e^- \rightarrow NO^-_{2\,\text{gas}} + O^- \quad (3)$$

In summary, we have successfully demonstrated TNT chemical sensing based on both SWNTs and ZnO nanowires. We have transferred aligned SWNTs onto cloth fabric and successfully fabricated flexible SWNT TNT

sensors, which can be used for wearable electronics. These flexible SWNT chemical sensors exhibited good sensitivity towards trace TNT molecules down to 8 ppb diluted with air as carrying gas, and the detection limit is comparable to conductive-polymer based TNT sensors. In addition, ZnO nanowire sensors were fabricated and the TNT detection limit was 60 ppb. A positive ion mass spectrometer was employed to understand the sensing mechanism, and revealed the presence of NO and NO_2 as decomposition products of TNT under room light irradiation. While the relative abundance of NO is believed to induce the conductance decrease for SWNT sensors, the reaction of NO with oxygen ions on ZnO nanowire surface can convert to NO_2 and lead to reduced conductance for ZnO nanowire sensor. The flexible TNT sensors could find immediate applications in systems that demand mechanical flexibility, light weight, and high sensitivity.

Experimental

The generation of diluted TNT vapor was carried out following reported literature.[46,47] For the demonstration of TNT sensing, 1.5 gram TNT powder (99.0% Chem Service) was placed in a 10 mL glass vial, which served as a reservoir of saturated vapor. A stream of dry air was used to transfer the TNT vapor out of the reservoir, and then was further diluted by another stream of dry air to obtain various concentrations. The air flow was directed toward the sensor surface, and the flow rates were controlled by mass flow controllers. The TNT concentration was calculated based on the saturated vapor pressure and the ratio of dilution, following ref. [23] Details can be found in the Supporting Information.

Acknowledgements

The authors P.-C.C., S.S., and K.R. contributed equally to this work. We thank Prof. Stephen B. Cronin and Mehmet Aykol for the use of the positive ion mass spectrometer and technical discussions. Supporting Information is available online from Wiley InterScience or from the author. This article is part of a Special Issue on USTC Materials Science.

Received: November 23, 2009
Published online: March 25, 2010

[1] Z. L. Wang, *Ann. Rev. Mater. Res.* **2004**, *55*, 159.
[2] A. Kolmakov, M. Moskovits, *Ann. Rev. Mater. Res.* **2004**, *34*, 151.
[3] J. G. Lu, P. Chang, Z. Fan, *Mater. Sci. Eng. R* **2006**, *52*, 49.
[4] E. S. Snow, F. K. Perkins, J. A. Robinson, *Chem. Soc. Rev.* **2006**, *35*, 790.
[5] P. C. Chen, G. Shen, C. Zhou, *IEEE Trans. Nanotech.* **2008**, *7*, 668.
[6] P. C. Chen, F. N. Ishikawa, H. Chang, K. Ryu, C. Zhou, *Nanotechnology* **2009**, *20*, 125503.
[7] V. V. Sysoev, J. Goschnick, T. Schneider, E. Strelcov, A. Kolmakov, *Nano. Lett.* **2007**, *7*, 3182.
[8] C. Richard, F. Balavoine, P. Schultz, T. W. Ebbesen, C. Mioskowski, *Science* **2003**, *330*, 775.
[9] Q. Cao, J. A. Rogers, *Adv. Mater.* **2009**, *21*, 29.
[10] E. S. Snow, F. K. Perkins, E. J. Houser, S. D. Badescu, T. L. Reinecke, *Science* **2005**, *307*, 1942.
[11] J. Kong, N. R. Franklin, C. Zhou, M. G. Chapline, S. Peng, K. Cho, H. Dai, *Science* **2000**, *287*, 622.
[12] P. Qi, O. Vermesh, M. Grecu, A. Javey, Q. Wang, H. Dai, *Nano Lett.* **2003**, *3*, 347.
[13] E. Comini, G. Faglia, G. Sberveglieri, Z. W. Pan, Z. L. Wang, *Appl. Phys. Lett.* **2002**, *81*, 1869.
[14] A. Kolmakov, D. O. Klenov, Y. Lilach, S. Stemmer, M. Moskovits, *Nano. Lett.* **2005**, *5*, 667.
[15] M. C. McApline, H. Ahmad, D. Wang, J. R. Heath, *Nature Materials* **2007**, *6*, 379.
[16] Q. H. Li, Y. X. Liang, Q. Wan, T. H. Wang, *Appl. Phys. Lett.* **2005**, *85*, 6389.
[17] H. Sohn, M. J. Sailor, D. Magde, W. C. Trogler, *J. Am. Chem. Soc.* **2003**, *125*, 3821.
[18] E. R. Goldman, I. L. Medintz, J. L. Whitley, A. Hayhurst, A. R. Clapp, H. T. Uyeda, J. R. Deschamps, M. E. Lessman, H. Mattoussi, *J. Am. Chem. Soc.* **2005**, *127*, 6744.
[19] J. P. Novak, E. S. Snow, E. J. Houser, D. Park, J. L. Stepnowski, R. A. McGill, *J. Am. Chem. Soc.* **2003**, *125*, 3821.
[20] F. Wang, H. Gu, T. M. Swager, *J. Am. Chem. Soc.* **2008**, *130*, 5392.
[21] C. Yu, Q. Hao, S. Saha, L. Shi, X. Kong, Z. L. Wang, *Appl. Phys. Lett.* **2005**, *86*, 063101.
[22] E. S. Snow, F. K. Perkins, *Nano Lett.* **2005**, *5*, 2414.
[23] C. Staii, A. T. Johnson, Jr. M. Chen, A. Gelperin, *Nano Lett.* **2005**, *5*, 1774.
[24] J. Li, Y. Lu, Q. Ye, M. Cinke, J. Han, M. Meyyappan, *Nano Lett.* **2003**, *3*, 929.
[25] S. Ju, Y. Xuan, P. Ye, D. B. Janes, F. Ishikawa, C. Zhou, G. Lu, A. Facchetti, T. J. Marks, *Nat. Nanotechnol.* **2007**, *2*, 378.
[26] K. Bradley, J. C. P. Gabriel, G. Gruner, *Nano Lett.* **2003**, *3*, 1353.
[27] S. J. Kang, C. Kocabas, T. Ozel, M. Shim, N. Pimparkar, M. A. Alam, S. V. Rotkin, J. A. Rogers, *Nat. Nanotechnol.* **2007**, *2*, 230.
[28] H.-J. Lim, D. Y. Lee, Y.-J. Oh, *Sens. Actuators A* **2006**, *125*, 405.
[29] S. Han, X. Liu, C. Zhou, *J. Am. Chem. Soc.* **2005**, *127*, 5294.
[30] C. Kocabas, S. Hur, A. Gaur, A. M. Meitl, M. Shim, J. A. Rogers, *Small* **2005**, *1*, 1110.
[31] F. N. Ishikawa, H. K. Chang, K. Ryu, P. Chen, A. Badmaev, L. De Arco Gomez, G. Shen, C. Zhou, *ACS Nano*, **2008**, *3*, 73.
[32] Q. Cao, H. S. Kim, N. Pimparkar, J. P. Kulkarni, C. J. Wang, M. Shim, K. Roy, M. A. Alam, J. A. Rogers, *Nature* **2008**, *454*, 495.
[33] D. Zhang, Z. Liu, C. Li, T. Tang, X. Liu, S. Han, B. Lei, C. Zhou, *Nano. Lett.* **2004**, *4*, 1919.
[34] C. Li, B. Lei, D. Zhang, X. Liu, S. Han, T. Tang, M. Rouhanizadeh, T. Hsiai, C. Zhou, *Appl. Phys. Lett.* **2003**, *83*, 4014.
[35] C. Li, D. Zhang, X. Liu, S. Han, T. Tang, S. Han, C. Zhou, *Appl. Phys. Lett.* **2003**, *82*, 1613.
[36] C. Li, D. Zhang, S. Han, X. Liu, C. Zhou, *J. of Phys. Chem. B* **2003**, *107*, 12451.
[37] D. Zhang, C. Li, X. Liu, S. Han, T. Tang, C. Zhou, *Appl. Phys. Lett.* **2003**, *83*, 1845.
[38] K. Ryu, D. Zhang, C. Zhou, *Appl. Phys. Lett.* **2008**, *92*, 93111.
[39] D. Zhang, C. Li, S. Han, X. Liu, T. Tang, W. Jin, C. Zhou, *Appl. Phys. A* **2003**, *77*, 163.
[40] T. R. Jeremy, F. K. Perkins, E. S. Snow, Z. Wei, P. E. Sheehan, *Nano Lett.* **2008**, *8*, 3137.
[41] G. W. Lemire, J. B. Simeonsson, R. C. Sausa, *Anal. Chem.* **1993**, *65*, 529.
[42] L. A. Pinnaduwage, A. Gehl, D. L. Hedden, G. Muralidharan, T. Thundat, R. T. Lareau, T. Sulchek, L. Manning, B. Rogers, M. Jones, J. D. Adams, *Nature* **2003**, *425*, 474.
[43] M. D. Bartberger, W. Liu, E. Ford, K. M. Miranda, C. Switzer, J. M. Fukuto, P. J. Farmer, D. A. Wink, K. N. Houk, *Proc. Natl. Acad. Sci. USA* **2002**, *99*, 10958.
[44] C. D. Schmelling, K. A. Gray, *Wat. Res.* **1995**, *29*, 2651.
[45] J. C. Oxley, J. L. Smith, Z. L. Zhou, R. L. Mckenney, *J. Phys. Chem.* **1995**, *99*, 10383.
[46] H.-J. Lim, D. Y. Lee, Y.-J. Oh, *Sens. Actuators A* **2006**, *125*, 405.
[47] S. Tao, G. Li, *Colloid Polym. Sci.* **2007**, *285*, 721.